Scaling in temporal occurrence of quasi-rigid-body vibration pulses due to macrofractures

G. Niccolini, A. Schiavi, and P. Tarizzo
Istituto Nazionale di Ricerca Metrologica, Strada delle Cacce 91, 10135 Turin, Italy

A. Carpinteri, G. Lacidogna, and A. Manuello
Department of Structural Engineering, Politecnico di Torino, Corso Duca degli Abruzzi 24, 10129 Torino, Italy

(Received 12 May 2010; revised manuscript received 24 September 2010; published 22 October 2010)

We subjected the time series of quasi-rigid-body vibration pulses (elastic emissions) from laboratory fracture carried out by a piezoelectric accelerometer on concrete and rock specimens under uniaxial compression to statistical analysis. In both cases, we find that the waiting-time distribution can be described by a scaling law extending over several orders of magnitude. This law is indistinguishable from a universal scaling law recently proposed for the waiting-time distributions of acoustic emissions in heterogeneous materials and earthquakes, suggesting its general validity for fracture processes independent of modes and magnitude scales.

DOI: 10.1103/PhysRevE.82.046115 PACS number(s): 89.75.Da, 05.65.+b, 43.40.Le, 62.20.mj

I. INTRODUCTION

Fracture in stressed-strained heterogeneous materials occurs as the culmination of progressive damage, which is accompanied by the spontaneous release of stored strain energy in the form of transient elastic waves [acoustic emission (AE)] [1–8]. Numerous investigations established that AE phenomenon varies while materials experience evolving damage [9–11]. Examples include two major damage mechanisms in composite materials—matricial cracks and decohesion between fiber and matrix—characterized by different AE amplitude distributions and rates [12]. Furthermore, AE energy released in different stages of damage process is concentrated in different sections of the frequency range. In particular, the observed frequency drop in the late stages of damage suggests the transition from microcracking regime to large cracks formation, which eventually leads to the material failure. Recently, a distinction between high-frequency and low-frequency AE, the latter called elastic emission (ELE), has been proposed [11]. ELEs are defined as AEs whose half-wavelengths are greater than the maximum size of propagation medium. This is a remarkable issue since an ELE event would imply a rigid vibration of the body, while high-frequency AEs are purely vibration modes of the body, including longitudinal (P), shear (S), and surface (Rayleigh) waves, due to microcrack growth [4,9]. Actually, ELEs are quasi-rigid-body vibrations resulting from the specimen flexibility and the constraints (specimen-platen contact with friction). The propagation of macrocracks, revealed by large stress drops, is preceded by bursts of radially expanding dilatational pulses generated by crack opening. Here, the temporal evolution of these ELE pulses, which thus play the role of fracture precursors in concrete and rock specimens under compression, is analyzed. In particular, the validity of a universal scaling law found for high-frequency AE and for earthquakes is investigated also for the distribution of waiting times between such pulses.

II. DAMAGE MONITORING BY ACCELEROMETRIC TECHNIQUE

We investigate the fracture of a cubic concrete specimen (d=0.1 m, ρ=2200 kg/m^3, and minimum elastic wave velocity v=2100 m/s) and a Green Luserna Granite cylindrical specimen (base diameter d=0.05 m, height h=0.1 m, ρ=2480 kg/m^3, and v=2450 m/s) subjected to uniaxial compression at constant displacement rates of 0.5 μm s^{-1} for concrete and 1 μm s^{-1} for granite, using a servohydraulic press with a maximum capacity of 500 kN. The specimens adhere to the press platens without any coupling material (specimen-platen contact with friction).

We focus on low-frequency quasi-rigid-body vibrations (ELE) using a piezoelectric accelerometer working in the range of 1–10 kHz (thus, the corresponding half-wavelengths are longer than the specimens size). The ELE pulses are characterized by the output response of the calibrated accelerometer (charge sensitivity of 9.20 pC/m s^{-2}), expressed in mm s^{-2}. The data are acquired at a sampling rate of 44.1 kHz for the entire duration of the tests.

In order to filter out environmental background noise, we set the detection threshold at 40 dB (referred to 1 μm s^{-2}).

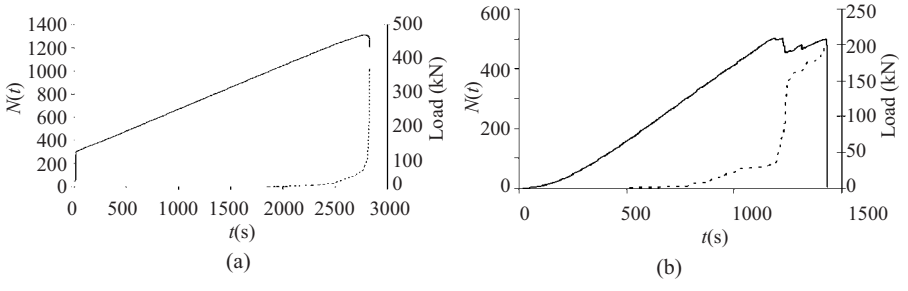

FIG. 1. Applied load (continuous line) and accumulated number of ELE events (dotted line) vs time for (a) concrete and (b) granite specimens, where failure is preceded by a significant load drop accompanied by a burst of ELE activity.

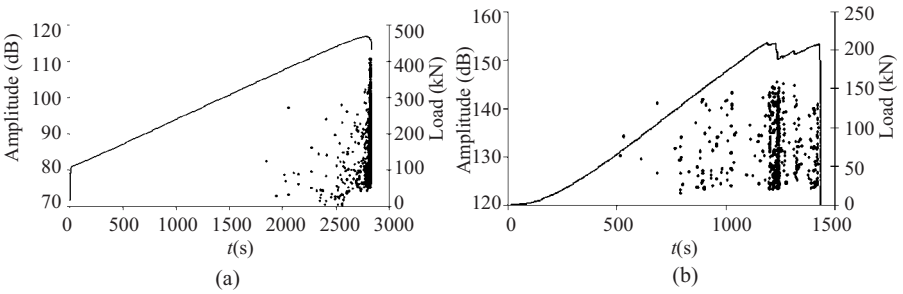

FIG. 2. Applied load and time series of ELE amplitudes in (a) concrete and (b) granite specimens. Increasing ELE activity in rate and amplitude precedes the final collapse and the intermediate load drops (granite).

In this way, we verify that no spurious signals are detected before the beginning of the test. Furthermore, we proceed to the identification and quantification of the mechanical noise of the press during the test.

The applied load on the concrete specimen and the accumulated number of detected ELE events as functions of time are reported in Fig. 1(a). The linearity of the load vs time—or displacement, being the test at constant displacement rate—curve characterizes a brittle behavior, where the specimen fails abruptly without any apparent accumulation of damage [13]. As a matter of fact, the failure is preceded by a sudden increase in the ELE activity, which is a signature of developing damage process.

The granite specimen is instead characterized by a nonlinear segment of the load vs displacement curve (quasibrittle behavior [13]), which is characterized by different load drops prior to the specimen failure [Fig. 1(b)]. Bursts of ELE activity precede the main load drops, suggesting propagation of large cracks before the specimen failure. In both cases, therefore, strong ELE activity announces serious structural damage, and it plays the role of fracture precursor.

The time series of ELE signals from concrete and rock specimens (Fig. 2) are subjected to time-frequency analysis, as shown in the two examples of Fig. 3; Fig. 3(a) presents a 60 s time window, during fracture experiment on concrete, characterized by signals with energy content concentrated in the frequency range from 3 to 6 kHz, while the 60 s time window in Fig. 3(b) contains signals emerging from the granite specimen with energy content spread over the range from 1 to 7 kHz.

The energy content of each ELE pulse is estimated by means of the spectral analysis of the local vibration velocity level, measured by the calibrated accelerometer attached at the specimen surface. Thus, the energy of ELE pulses ranges between 1.1×10^{-13} J (10^{-3} GeV) and 5.6×10^{-8} J (346 GeV) for concrete, and between 1.3×10^{-11} J (0.1 GeV) and 6.1×10^{-7} J (3.7×10^{3} GeV) for granite.

III. SCALING LAW FOR ELE WAITING-TIME DISTRIBUTIONS

The space-time organization of AE and earthquake source process is ruled by different scaling laws; among them, the most important are the Gutenberg-Richter (GR) law for the magnitude distribution [14] and the Omori law for the rate of aftershocks as a function of time from the main shock [15–21]. In particular, the GR law can be expressed in terms of the mean event rate, $R_{Mth}\equiv N(M_{th})/T=10^{a}\times10^{-bM_{th}}/T$, where $N(M_{th})$ is the number of events with magnitude $M\geq M_{th}$ occurring in a certain region during a sufficiently long period T.

Bak *et al.* introduced a different way to study earthquake waiting times [22]. Starting from this pioneer work, Corral [23] established that the distributions of waiting times between earthquakes follow a universal scaling law in different regions of the world and earthquake catalogs if rescaled by the mean rate R_{Mth}. The scaling law introduced by Corral for earthquake sequences [23,24], and later confirmed by the experiments on fracture phenomena [25–27], is a very important universal law of crackling phenomena, which has been recently recovered by theoretical investigations of creep rupture phenomena based on fiber bundle models [28,29]. The universal form of the scaling law is preserved also in the case of largely varying event rates—as, for example, during the presented experiments with periods dominated by pronounced ELE sequences prior to large stress drops (Fig. 3)—if instantaneous rates $r(t)$ are used instead of mean rates R [23,25].

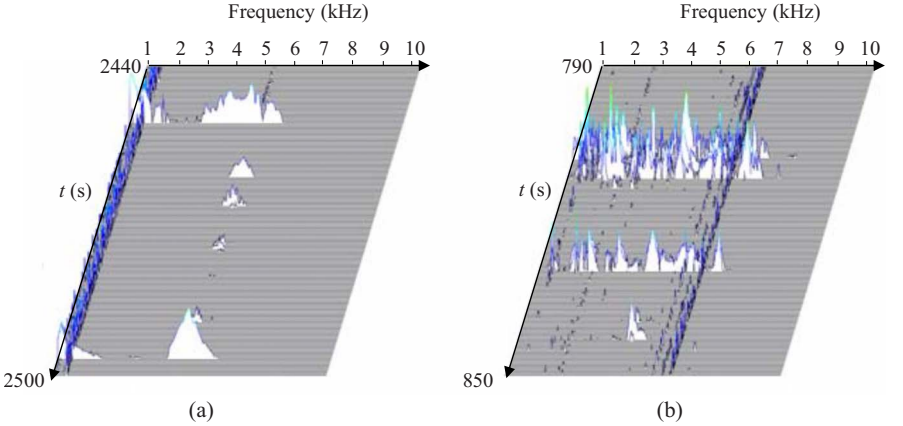

FIG. 3. (Color online) Spectral analysis of ELE activity in (a) concrete and (b) granite specimens.

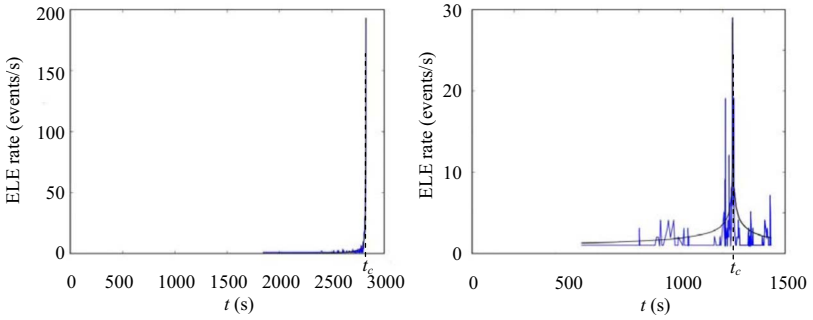

FIG. 4. (Color online) Instantaneous rate $r(t)_{Mth}$ for (a) concrete, $M_{th}=70$ dB, and (b) granite, $M_{th}=120$ dB, around the main shock (the highest peak in the ELE activity) fitted with the inverse and the direct Omori laws.

We extend this approach to concrete and granite ELE time series, focusing on two quantities to characterize each ELE event: time of occurrence, defined here by the time of the peak amplitude a_{max}, and magnitude, expressed in dB through the relation $M=20\log(a_{max}/1\ \mu\text{m s}^{-2})$.

We choose a minimum magnitude M_{th} for a given time series of ELE events (Fig. 3), in such a way that only the $N(M_{th})$ events with magnitude $M \geq M_{th}$ are taken into account. All the events with $M \geq M_{th}$ define a point process in time where events occur at t_i with $1 \leq i \leq N(M_{th})$, and therefore the waiting times can be obtained as $\tau_i \equiv t_i - t_{i-1}$. For each threshold M_{th}, the probability density function (PDF) of waiting times τ is denoted by $p_{Mth}(\tau)$.

Therefore, the PDFs of rescaled waiting times $\theta_i \equiv r(t_i)_{Mth}\tau_i$ from concrete and granite time series are obtained for several M_{th} values, where the instantaneous rate $r(t)_{Mth}$ for events with $M \geq M_{th}$ is defined by the direct and the inverse Omori laws introduced in seismicity [15,16], which characterize also foreshock and aftershock AE sequences with respect to the specimen failure [17–20]. The inverse Omori law is applied here to describe the power-law increase in the ELE rate (foreshocks sequence) prior to the highest rate (main shock, which coincides with a critical load drop), increasing on average as a power law. More precisely, $r(t)_{Mth}=r_{0,Mth}/[1+(t_c-t)/c']^{p'}$, where t_c-t is the time to the main shock occurring at t_c, and $r_{0,Mth}$ is the highest rate for $M \geq M_{th}$ (strength of the main shock). The parameters c' and p' are magnitude dependent as well; for example, the Omori law increase in concrete ($M_{th}=70$ dB) and in granite ($M_{th}=120$ dB), respectively, yields $p'=1$, $c'=1.2$ and $p'=0.4$, $c'=0.2$ (Figs. 4 and 5). Similarly, the power-law decay in the ELE rate after the main shock in granite specimen is described by the direct Omori law $[1+(t-t_c)/c]^{-p}$, with $p=0.5$ and $c=0.6$.

The observed deviations from the fitting Omori law, especially in the case of the aftershock sequence in granite, are probably due to the fact that laboratory tests typically produce more foreshock than aftershock events, contrary to the case observed in seismicity data [21]. Another potential reason is that the two Omori laws refer to standard AE measurements and not specifically to ELE events, which thus could behave differently. Related issues are the difficulty in resolving separate events (overlapping) and the missing low-amplitude events hidden in sequences of higher-amplitude events. This fact accounts for the deficit of short waiting times already observed in the earthquake distributions [22], which is a potential problem also for the ELE analysis on laboratory specimens.

Both sets of rescaled distributions exhibit data collapse (shown in Fig. 6), which illustrates the fulfillment of a scaling law:

$$p_{Mth}(\tau) = r(t)_{Mth} f[r(t)_{Mth}\tau]. \tag{1}$$

Thus, for a given threshold M_{th}, $p_{Mth}(\tau)$ is determined by its rate $r(t)_{Mth}$ and the scaling function f, which can be well approximated by a gamma function:

$$f(\theta) \propto \theta^{-(1-\gamma)} \exp(-\theta/x), \tag{2}$$

where $\theta \equiv r(t)_{Mth}\tau$ is the rescaled waiting time.

As the scaling function f is introduced in such a way that the mean of θ is $\langle\theta\rangle=1$, the parameters are not independent; for normalization constant=1, $\langle\theta\rangle=\gamma x$ and therefore $\gamma=1/x$. Thus, essentially, there is only one parameter to fit.

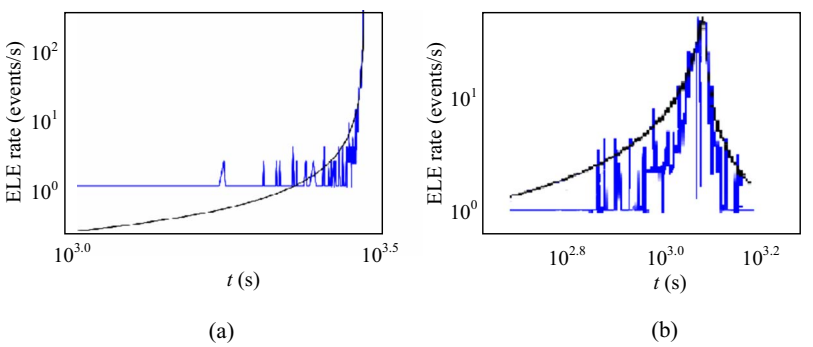

FIG. 5. (Color online) Instantaneous rate $r(t)_{Mth}$ for (a) concrete, $M_{th}=70$ dB, and (b) granite, $M_{th}=120$ dB, in a log-log scale.

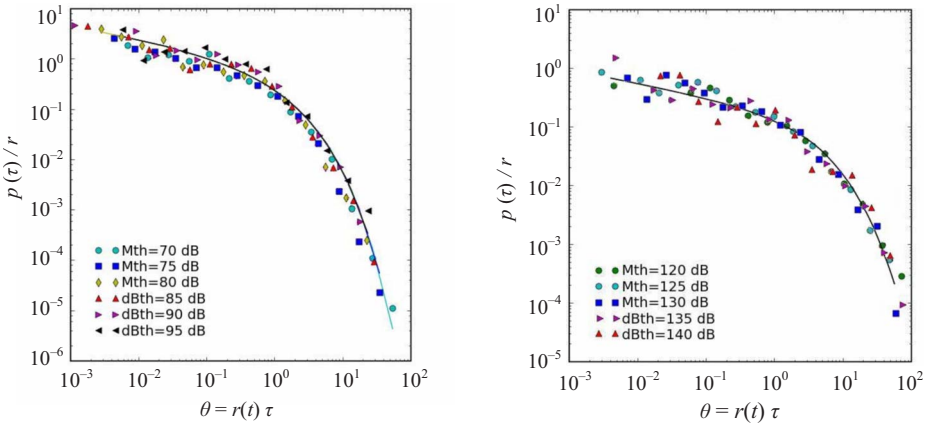

(a) (b)

FIG. 6. (Color online) Probability density functions of the rescaled waiting times $\theta \equiv r(t)\tau$ for ELE events in (a) concrete and (b) granite. The solid line is the fitting function defined in Eq. (2).

The fit yields $\gamma = 0.73 \pm 0.07$ and $x = 1.56 \pm 0.76$ for concrete, and $\gamma = 0.79 \pm 0.09$ and $x = 1.36 \pm 0.64$ for granite. Therefore, we observe a slow power-law decay with exponent $1 - \gamma = 0.2 - 0.3$ up to $\theta \approx 1$, followed by a faster exponential decay for larger values of the argument. Both scaling collapses are statistically indistinguishable and in remarkable agreement with recent findings for earthquakes [23,24] and high-frequency AE in rock [25] and concrete [26,27] specimens ($\gamma \approx 0.7$ and $x \approx 1.5$). This indicates that the universal scaling function describing the waiting-time distribution is still valid for these quasirigid vibration modes. In the present case study, the range of validity of the scaling law extends over six orders of magnitude, from the largest fractures of estimated ELE released energy of $\sim 10^{-7}$ J down to the smallest ones with energy smaller than 10^{-13} J.

IV. CONCLUSIONS

Statistical analysis of the temporal features of noise accompanying fracture of heterogeneous materials is carried out by means of the acoustic-emission technique on concrete and rock specimens under uniaxial compression. The use of a piezoelectric accelerometer working the frequency range (1–10 kHz) leads to the detection of low-frequency quasirigid body vibration pulses. The waiting-time distribution of these particular modes, also called ELEs, is described by a scaling law which is compatible with the one recently established for high-frequency acoustic emissions and earthquakes. The energy of these pulses, emitted from large cracks preceding the specimen failure, is found to extend over six orders of magnitude, from $\sim 10^{-7}$ J down to $\sim 10^{-13}$ J, while the scale of waiting times extends from $\sim 10^{-2}$ to 10^{2} s.

[1] C. H. Scholz, J. Geophys. Res. **73**, 1417 (1968).
[2] D. A. Lockner, J. D. Byerlee, V. Kuksenko, A. Ponomarev, and A. Sidorin, Nature (London) **350**, 39 (1991).
[3] D. Lockner, Int. J. Rock Mech. Min. Sci. Geomech. Abstr. **30**, 883 (1993).
[4] M. Ohtsu, Mag. Concrete Res. **48**, 321 (1996).
[5] A. Guarino, A. Garcimartin, and S. Ciliberto, Eur. Phys. J. B **6**, 13 (1998).
[6] A. Carpinteri, G. Lacidogna, G. Niccolini, and S. Puzzi, Meccanica **43**, 349 (2008).
[7] H. R. Hardy, in *Acoustic Emissions in Geotechnical Engineering Practice*, edited by V. P. Drnevich and R. E. Gray, STP No. 750 (American Society for Testing Materials, Baltimore, 1981), pp. 4–92.
[8] K. Mogi, Bull. Earthquake Res. Inst., Univ. Tokyo **40**, 831 (1962).
[9] H. L. Dunegan, J. Acoust. Emiss. **15**, 1 (1998).
[10] G. I. Kukalov and G. E. Yakovitskaya, Mining Institute, Siberian Branch, Russian Academy of Sciences, Novosibirsk **2**, 111 (1993).
[11] A. Schiavi, G. Niccolini, P. Tarizzo, G. Lacidogna, and A. Carpinteri, Strain, doi: 10.1111/j.1475-1305.2010.00745.x (2010).
[12] M. Bruneau and C. Potel, *Materials and Acoustic Handbook* (ISTE, London/Wiley, Hoboken, NJ, 2009), Chap. 24.
[13] D. Krajcinovic, *Damage Mechanics* (Elsevier, Amsterdam, 1996).
[14] C. F. Richter, *Elementary Seismology* (Freeman, San Francisco, 1958).
[15] F. Omori, J. Coll. Sci., Imp. Univ. Tokyo **7**, 111 (1894).
[16] T. Utsu, Y. Ogata, and S. Matsu'ura, J. Phys. Earth **43**, 1 (1995).
[17] C. H. Scholz, Bull. Seismol. Soc. Am. **58**, 1117 (1968).
[18] A. Helmstetter and D. Sornette, Phys. Rev. E **66**, 061104 (2002).
[19] T. Hirata, J. Geophys. Res. **92**, 6215 (1987).
[20] O. Ojala, I. G. Main, and E. B. T. Ngwenya, Geophys. Res. Lett. **31**, L24617 (2004).
[21] I. G. Main, Geophys. J. Int. **142**, 151 (2000).
[22] P. Bak, K. Christensen, L. Danon, and T. Scanlon, Phys. Rev. Lett. **88**, 178501 (2002).
[23] A. Corral, in *Modelling Critical and Catastrophic Phenomena*

in Geoscience: A Statistical Physics Approach, edited by P. Bhattacharyya and B. K. Chakrabarti, Lecture Notes in Physics Vol. 705 (Springer, Berlin, 2006), pp. 191–221.

[24] J. Davidsen and C. Goltz, Geophys. Res. Lett. **31**, L21612 (2004).

[25] J. Davidsen, S. Stantchis, and G. Dresen, Phys. Rev. Lett. **98**, 125502 (2007).

[26] G. Niccolini, G. Durin, A. Carpinteri, G. Lacidogna, and A. Manuello, J. Stat. Mech.: Theory Exp. (2009), P01023.

[27] G. Niccolini, F. Bosia, A. Carpinteri, G. Lacidogna, A. Manuello, and N. Pugno, Phys. Rev. E **80**, 026101 (2009).

[28] F. Kun, H. A. Carmona, J. S. Andrade, and H. J. Herrmann, Phys. Rev. Lett. **100**, 094301 (2008).

[29] F. Kun, Z. Halz, J. S. Andrade, Jr., and H. J. Herrmann, J. Stat. Mech.: Theory Exp. (2009), P01021.